Vol. 38, No. 4 (2016) 552-558

Tribology in Industry

www.tribology.fink.rs

RESEARCH

Effect of Composition on Mechanical Properties of Mullite-WC Nano Composites Prepared by Spark Plasma Sintering

H. Rajaei[a], I. Mobasherpour[a], M. Farvizi[a], M. Zakeri[a]

[a] *Ceramics Department, Materials and Energy Research Center, Karaj, Iran.*

Keywords:

Mullite
WC
Nano composite
Spark plasma sintering

Corresponding author:

Iman Mobasherpour
Ceramics Department, Materials and Energy Research Center, Karaj, Iran.
E-mail:Iman.Mobasherpour@gmail.com

A B S T R A C T

Mullite-WC composites were prepared from Mullite and WC powders by spark plasma sintering at 1400 °C for a holding time of 180 s under 30 MPa. Microstructure, strength, and hardness of the mullite-WC composites were studied. The mullite-WC composite containing 5-20 wt% WC reached over 94 % theoretical density. The strength and Vickers hardness of mullite-(10 wt%) WC sintered composite reached maximum values of 298 MPa, and 1589 HV, respectively demonstrating that the introduction of WC significantly enhances the mechanical properties of the mullite matrix.

1. INTRODUCTION

During the recent decades, researchers conducted extensive studies on ceramics based composites and nano composites [1–11]. Results established that for reinforced ceramics, the creep rate is lower by two up to three orders of magnitude, and the strength is higher by two up to three times compared to the ceramics without reinforcements [2,3,5,8].

Nevertheless, fabrication of dense composites is a challenge because the reinforcing phases are often carbides, nitrides or borides, which are very difficult to densify. On top of that, there have been a lot of difficulties in achieving a uniform dispersion of reinforcing phases in the matrix. Agglomeration of reinforcing particles can markedly deteriorate the densification and degrade the properties of the produced composites. The processing difficulties are aggravated when reinforcing phases are sub micrometer or nanometer sized powders because finer particles tend to form stronger agglomerates [12].

Mullite ($3Al_2O_3.2SiO_2$) has been considered a good candidate for high temperature application [13] because of its marvelous properties, such as good chemical and thermal stability, low thermal expansion and conductivity coefficient, low dielectric constant and high creep resistance [14]. However, application of mullite is largely limited because of its rather low strength and fracture toughness [14]. Continuous reinforced mullite matrix composites have been extensively

investigated recently in order to improve the inherent brittleness of monolithic mullite ceramic [15-19]. Continuous silicon carbide fiber- or aluminosilicate reinforced mullite matrix composites have been used in advanced applications, such as aero engines, stationary gas turbines and heat exchangers [20]. Nevertheless, these mullite composites are not much reliable at temperatures higher than 1500 °C because of the severe degradation of silicon carbide or aluminosilicate phases [21].

Tungsten carbide (WC) is a superior candidate as second phase material and it is extensively used in cutting tools and protective coatings because of its unique combination of properties viz. high melting temperature, extremely hard, chemical stability, excellent abrasive and corrosion resistance [22].

Spark plasma sintering (SPS) or plasma pressure compaction is a technique for densifying any class of materials, especially those that are difficult to be sintered by the conventional techniques [23]. Presence of plasma in spark plasma sintering systems is still unproven. Specific advantages of SPS over the conventional sintering techniques are: (1) a faster heating rate, which avoids mass transport mechanisms that do not contribute to the densification (2) a shorter dwell time, which retains finer microstructures, and (3) DC pulse voltage, which contributes to an enhanced mass transport through electro-migration [24].

In this study, SPS technique was used to prepare mullite-WC composites, and influence of composition on microstructures and mechanical properties of composites was investigated.

2. EXPERIMENTAL PROCEDURE

2.1 Materials

WC powder was provided by Alfa Aesar Co. (Art No.12070). Figure 1 shows a SEM image of the pure WC powder. As can be seen, it consist WC particles exhibiting severe initial agglomeration. Particle size distribution analysis was performed for the WC powder by the dynamic laser scattering technique using Fritsch particle sizer analysts. It can be found from Fig. 2 that the mean particle size (D50) of the powder was 3.20 μm, and the number percentage of the particles below 9 μm was 90 %.

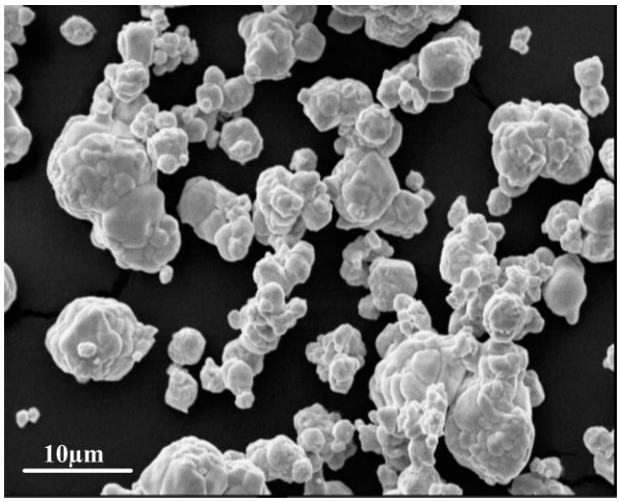

Fig. 1. Scanning electron micrographs of primarily WC powder.

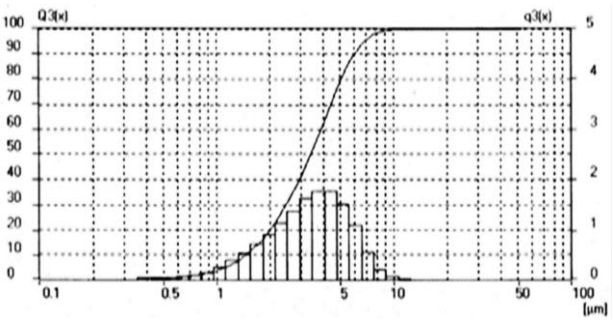

Fig. 2. Particle size analyses of WC powder.

A fine mullite ($3Al_2O_3.2SiO_2$) powder was synthesized by sol-gel process using aluminum nitrate (Art No. 101086, Merck Co.) and tetra ethyl ortho silicate (TEOS) (Art No. 800658, Merck Co.) as starting materials. The detailed synthesis procedure is reported in literature [25].

Phase identification of the synthesized mullite powders were performed by X-ray diffraction (XRD) method using a Cu–K_α, Siemens diffractometer. Particle size of the synthesized mullite powder was obtained by field emission scanning electron microscopy (FE-SEM Mira 3-XMU).

2.2 SPS operation

WC and mullite powders were mixed by a ball mill to produce mullite-WC (0-20 wt%) mixtures. The wet milling was performed in a plastic vial for 12 h at a speed of 200 rpm in presence of 50 ml ethanol. The mixed powders

were dried and then passed through a sieve with a pore-opening size of 100 μm. Using a graphite die with an inner diameter of 50 mm, Powders were sintered by an SPS machine (SPS-20T-10, Easy fashion metal products trade Co.). Standard DC pulse ON–OFF sequence with current 2.6 kA was chosen for all the experiments. The heating rate was 1 °C/s and sintering was performed under vacuum at a temperature of 1400 °C for a holding time of 180 sec with pressure 30 MPa. The temperature of die was measured by an optical pyrometer.

2.3 Characterization

Siemens diffract meter with Cu K_α radiation (λ = 0.1541 nm) was used to study the phase evolution of sintered samples. Diffraction measurements were performed at 30 kV /20mA with scanning speed of 1 °/min for scanning range of 20–80° with intervals of 0.02°. Morphology of synthesized mullite and microstructure evolution of sintered samples were investigated by a field emission scanning electron microscopy (FE-SEM) Mira 3-XMU operating at 30 kV and scanning electron microscopy (SEM) ZEISS operating at 15 kV, respectively.

Using distilled water, ASTM C373-88 standard via Archimedes method was applied in order to study changes in the density of samples. The mean density values were obtained by averaging values of densities of three specimens for each composition. Theoretical densities of mullite (3.05 g/cm^3), and WC (15.63 g/cm^3) were used to calculate relative densities.

Following ASTM-C1327-08 standard, the Vickers hardness was measured using a micro hardness tester (MVK-H21, Akashi Co.) with a load of 1 kg for a holding time of 15 sec. Surface of samples was prepared for the hardness tests through polishing with 1μm diamond slurry. 5 measurements for each sample were averaged to evaluate Vickers hardness. Specimens with dimensions of 20mm×4mm×2mm were cut and machined for bending strength tests according to ASTM C1161-13. The entire specimen surface was ground by an 800-grit diamond wheel and surface facing to the tensile machine was polished by diamond slurries. Bending strength of samples was measured at room temperature by a three-point bending test operating with a crosshead speed of 0.5 mm/min. For each set of compositions, at least five specimens were tested for both strength and hardness measurements.

3. RESULTS AND DISCUSSION

3.1 Characterization of mullite

Morphology of synthesized mullite single particles is shown in Fig. 3. The particles have a spindle-like morphology with an average particle size in the range of 80–200 nm. Figure 4 shows XRD pattern of synthesized mullite powder compacted at elevated temperature. Mullite is main phase in the specimen sintered at 1400 °C and diffraction peaks of γ-Al_2O_3, Al or Si-spinel not be observed in pattern.

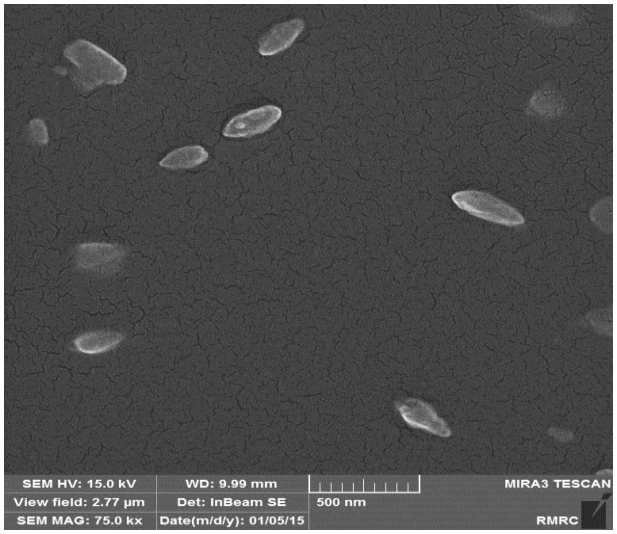

Fig. 3. Scanning electron micrographs of synthesized mullite powder.

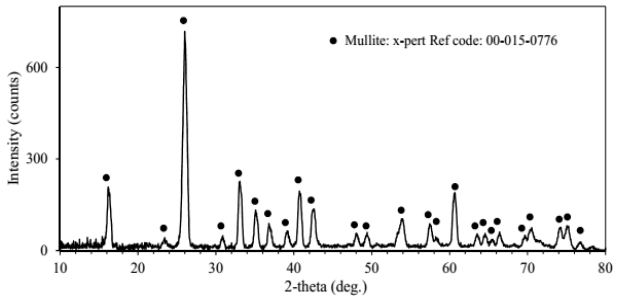

Fig. 4. XRD of synthesized mullite powder compact at elevated temperature.

3.2 Effect of composition

Figure 5 shows XRD patterns of the mullite-WC (5, 10, 15, and 20 wt.%) composites sintered at

1400 °C for a sintering time of 180 sec. Patterns reveal the presence of only mullite and WC phases, which indicates that there was no reaction between mullite and WC during milling or sintering process. This finding is similar to the results reported in literature for Al_2O_3-WC [26], and mullite-TiC [19] composites.

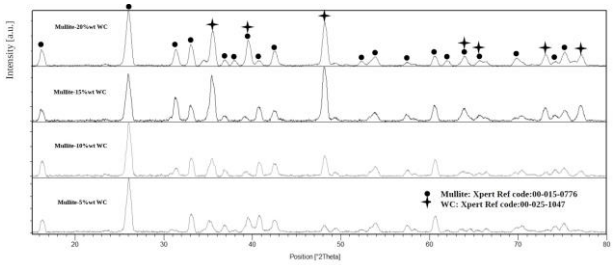

Fig. 5. XRD pattern of Mullite-(5 %wt) WC, Mullite-(10 %wt) WC, Mullite-(15 %wt) WC and Mullite-(20 %wt) WC sintered at 1400°C for 180s.

Table 1. Relative densities and mechanical properties of various Mullite-WC composite samples that were analyzed after sintered at 1400 °C for 180 s by SPS.

Composition	Relative density (%)	Bending strength (MPa)	Hardness (HV)
Mullite	94.1	220	1269
Mullite-(5 wt%) WC	94.6	235	1528
Mullite-(10 wt%) WC	96	298	1589
Mullite-(15 wt%) WC	95.5	273	1568
Mullite-(20 wt%) WC	95.1	245	1536

It is well known that mullite has very poor sinter ability and could be sintered to full density only at temperature higher than 1700 °C [27–29]. Table 1 shows relative densities and mechanical properties of sintered mullite-WC samples.

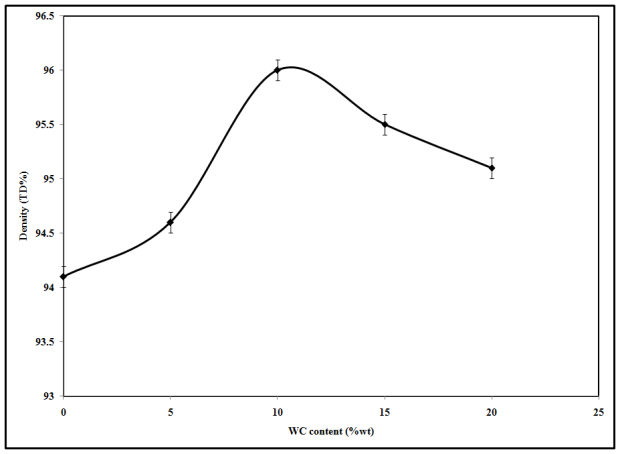

Fig.6. Sintering curves of Mullite-WC composite powder.

Figure 6 shows the effect of content WC on relative density of sintered composites. Considering Fig. 6 and table 1, one can realize the sintering behavior of the mullite-WC composites with different compositions. Despite the detrimental effect of the presence of WC phase on sintering, all of samples have reached over 94 % of their theoretical density (TD). Mullite-10 wt% WC sample reached the highest relative density compared to other compositions.

Contact points between particles are highly resistant to current flow and contribute to an increased heating. The temperature at those localized heating zones exceeds melting temperature of material. The cumulative effect from all such zones results in an improved densification at rather lower sintering temperatures compared to conventional sintering techniques [18]. The effectiveness of low temperature sintering in SPS can be explained as follows: Firstly during spark plasma sintering, high heating rate enables sample to skip over the low-temperature regime where the nondensifying mechanism (surface diffusion) is active and sample proceeds directly into the elevated temperature regime where densifying mechanisms predominate. Thus, SPS suppresses the grain pre coarsening before actual sintering starts [30]. Secondly, electric discharge, electric shock pressure and mechanical pressure during SPS also improve mass transport between ceramic particles and thus sintering progress is significantly better in SPS compared to the pressure less sintering and even hot pressing methods [31, 32].

Figure 7 shows, SEM micrographs of polished cross section of mullite-WC composites containing 5, 10, 15 and 20 wt% sintered at 1400 °C for 180 sec. Due to rather low sintering temperature, short sintering time and pining effect of the WC particles on grain growth of mullite matrix, a fine matrix grained microstructure is observed for composites with different amount of WC. The microstructure is homogeneous and WC particles are present inside at the grain boundaries. As Fig. 7c shows, WC is well uniformly distributed in mullite matrix. Figure 7b shows that microstructure of mullite-(10 wt%) WC sintered composites is better densified and contains less pores in comparison with the other composites.

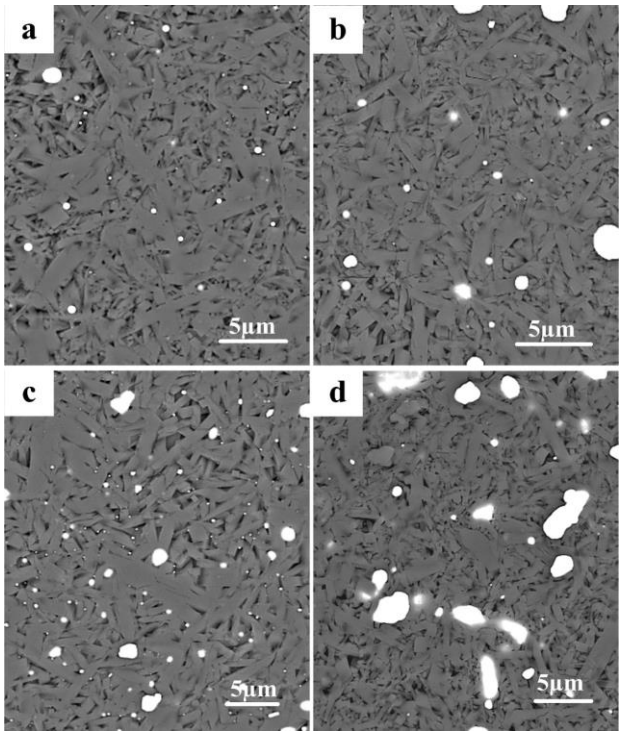

Fig. 7. SEM micrographs of Mullite-WC composites: (a) Mullite-(5 %wt) WC; (b) Mullite-(10 %wt) WC; (c) Mullite-(15 %wt) WC; (d) Mullite-(20 %wt) WC sintered at 1400 °C for 180s by SPS.

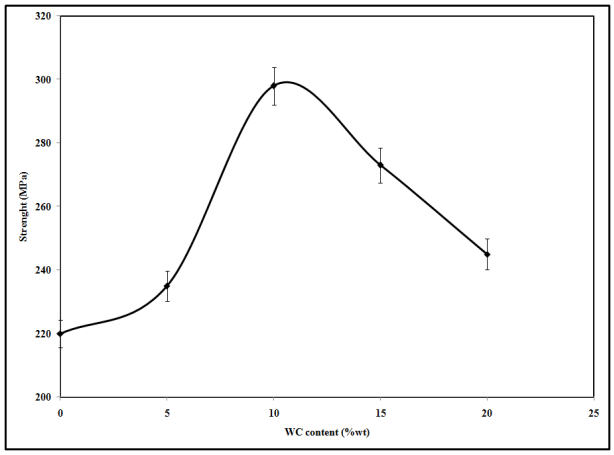

Fig. 8. Plots of effect composition on the strength of Mullite-WC composite.

Figure 8 shows, effect composition on strength of mullite-WC composites. The strength increases steadily by increasing WC content up to 10 wt%. The strength of mullite-WC (5, 10, 15 and 20 wt%) composites reach 235 MPa, 298 MPa, 273MPa and 245 MPa, respectively. In comparison with rather poor strength of the monolithic mullite sintered by conventional sintering method (≈200 MPa) [33], and the monolithic mullite sintered by SPS (≈220 MPa), the strength of present mullite-WC composites is significantly improved. The increase in Young's modulus [33], refinement of microstructure and residual stress strengthening effects resulted by the presence of WC particles in the matrix are the important factors that improve strength. Besides, formation of dislocation networks in the matrix and the strengthening by grain boundaries also contribute to increase in strength [2,3]. According to Fig. 7, by increase of WC content more than 10 wt% up to 20 wt% the agglomeration of WC particle occurred. Duos to rather high sintering temperature of WC, the agglomeration of WC phases and increase of porosity have detrimental effect on sintering behavior and mechanical properties.

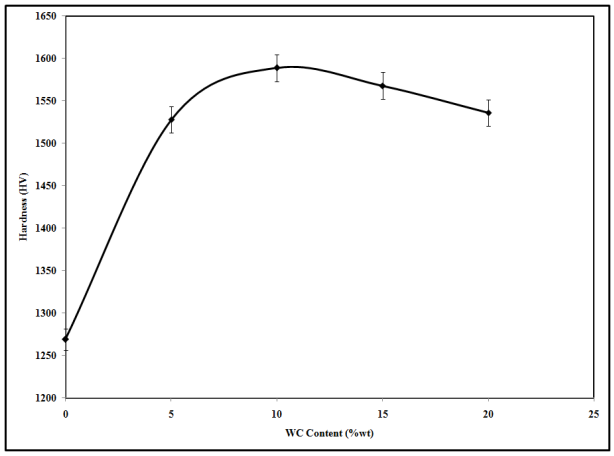

Fig. 9. Effect of WC content on the Vickers hardness of Mullite-WC composite sintered at 1400 °C for 180 s by SPS.

Figure 9 shows Vickers hardness of sintered mullite-WC composites. Mullite-10 wt. % WC composite achieved the highest hardness value of 1589 HV. The high hardness of WC particles dispersed in mullite matrix caused an increase in hardness. Hardness values for composite materials ranged between 15.3 and 15.9 GPa, which are significantly improved compared to that of pure mullite (12.7 GPa). The hardness values of mullite-WC composites in the present study are comparable with values reported in literature for alumina-WC [6], and mullite-TiC [19] composites. The hardness of sintered mullite-WC composites decreases with an increase in WC content over 10 wt%. This decrease in hardness is explained by the lowering relative density of mullite-WC (15 or 20 wt%) composites (Fig. 6).

4. CONCLUSION

Spark plasma sintering of mullite-WC composite powders was investigated. The sinterability of

composites increased steadily by increasing WC content up to 10 wt%. Because of suppressed grain coarsening and enhanced mass transport by electric discharge, highly densified mullite-WC composites were produced at 1400 °C by SPS. Composite with WC content of 5-20 wt% have reached over 94 % of their theoretical density. The strength and Vickers hardness of mullite-WC (10 wt%) composite sintered at 1400 °C had a maximum value of 298 MPa and 1589 HV, respectively. The strength and hardness of sintered mullite-WC composites decrease by an increase in WC content over 10 wt%.

REFERENCES

[1] A. Mukhopadhyay and B. Basu, 'Consolidation–microstructure–property relationships in bulk nanoceramics and ceramic nanocomposites: a review', *Int. Mater. Rev.*, vol. 52, no. 5, pp. 257-288, 2007.

[2] K. Niihara, A. Nakahira and T. Sekino, 'New Nanocomposite Structural Ceramics', Materials Research Society Symposium Proceedings, vol. 286, pp. 406–413, 1993.

[3] K. Niihara, 'New Design Concept of Structural Ceramics (Ceramic Nanocomposites)', *J. Ceram. Soc. Jpn.*, vol. 99, no. 1154, pp. 974–982, 1991.

[4] J.H. Zhao, C.S. Laura, P.H. Martin, M.C. Helen and A.M. Gary, 'Mechanical Behavior of Alumina–Silicon Carbide (Ceramic Nanocomposites)', *J. Am. Ceram. Soc.*, vol. 76, no. 2, pp. 503–510, 1993.

[5] U. Hisao, T. Hidekazu, T. Takeyoshi, N. Atsushi and N. Koichi, 'Pressureless Sintering of Al_2O_3/TiC Nanocomposites', *Powder Metall*., vol. 41, no. 10, pp. 1226–1231, 1994.

[6] A. Nakahira, K. Niihara, 'Sintering Behaviours and Consolidation Process for Al_2O_3/SiC Nanocomposites', *J. Ceram. Soc. Jpn*., vol. 100, no. 4, pp. 448-453, 1992.

[7] L. Gao, H.Z. Wang, J.S. Hong, H. Miyamoto, K. Miyamoto, Y.Nishikawa and D. De la Torre, 'SiC-ZrO_2(3Y)-Al_2O_3 nanocomposites superfast densified by spark plasma sintering', *Nanostruct. Mater*., vol. 11, no. 1, pp. 43–49, 1999.

[8] Y. Eiichi, Q.L. Bao and K. Niihara, 'The Effects of Fine SiC Particles on the Creep of MgO at High Temperatures', *J. Ceram. Soc. Jpn*., vol. 100, no. 1160, pp. 514–519, 1992.

[9] W.Q. Li and L. Gao, 'Processing, microstructure and mechanical properties of 25 vol% YAG-Al_2O_3 nanocomposites', *Nanostruct. Mater*., vol. 11, no. 8, pp. 1073–1080, 1997.

[10] L. Gao, H.Z. Wang, J.S. Hong, H. Miyamoto, K. Miyamoto, Y. Nishikawa and S. Torre, 'Mechanical Properties and Microstructure of Nano-SiC-Al_2O_3 Composites Densified by Spark Plasma Sintering', *J. Eur. Ceram. Soc*., vol. 19, no. 5, pp. 609–613, 1999.

[11] H.Z. Wang, L. Gao and J.K. Guo, 'Fabrication and Microstructure of Al_2O_3-ZrO_2(3Y)-SiC Nanocomposites', *J. Eur. Ceram. Soc*., vol. 19, no. 12, pp. 2125–2131, 1999.

[12] Y.J. Lin and C.P. Tsang, 'Fabrication of mullite/SiC and mullite/zirconia/SiC composites by 'dual' in-situ reaction syntheses', *Mater. Sci. Eng., A*, vol. 344, no. 1-2, pp. 168-174, 2003.

[13] T.R. Prabhu, 'Airworthiness Certification of Fe-Si3N4-graphite Brake Composites for Military Aircraft', *Tribology in Industry*, vol. 37, no. 4 pp.491-499, 2015.

[14] Y. Wang, H. Cheng and J. Wang, 'Effects of the single layer CVD SiC inter phases on mechanical properties of mullite fiber-reinforced mullite matrix composites fabricated via a sol– gel process', *Ceram. Int*., vol. 40, no. 3, pp. 4707–4715, 2014.

[15] Z.I. Zaki, Nasser Y.Mostafa and Y.M.Z. Ahmed, 'Synthesis of dense mullite/$MoSi_2$ composite for high temperature applications', *Int. J. Refract. Met. Hard Mater*, vol. 45, pp. 23-30, 2014.

[16] K.K. Chawla, 'Interface engineering in mullite fiber/mullite matrix composites', *J. Eur. Ceram. Soc.,* vol. 28, no. 2, pp. 447–453, 2008.

[17] F.W. Zok, 'Developments in oxide fiber composites', *J. Am. Ceram. Soc*., vol. 89, no. 11, pp. 3309–3324, 2006.

[18] D. Ghahremani, T. Ebadzadeh and A. Maghsodipour, 'Spark plasma sintering of mullite: Relation between microstructure, properties and spark plasma sintering (SPS) parameters', *Ceram. Int.*, vol. 41, no. 5, pp. 6409-6416, 2015.

[19] D. Ghahremani, T. Ebadzadeh and A. Maghsodipour, 'Densification, microstructure and mechanical properties of Mullite–TiC composites prepared by spark plasma sintering', *Ceram. Int*., vol. 41, no. 2, pp. 1957-1962, 2015.

[20] M.A. Mattoni, J.Y. Yang, C.G. Levi and F.W. Zok, 'Effects of combustor rig exposure on a porous-matrix oxide composite', *Int. J. Appl. Ceram. Technol*., vol. 2, no. 2, pp. 133–140, 2005.

[21] H. Schneider, J. Schreuer and B. Hildman, 'Structure and properties of mullite – a review', *J. Eur. Ceram. Soc.*, vol. 28, no. 2, pp. 329–344, 2008.

[22] K.N. Pramoda, L. Hao-Tung, C. Man-Ping, C. Wei-Hsio and H. Jow-Lay, 'Microstructure analysis and mechanical properties of a new class of Al_2O_3–WC nanocomposites fabricated by spark plasma sintering', *J. Eur. Ceram. Soc*., vol. 33, no. 15-16, pp. 3095-3100, 2013.

[23] A. Lanzutti, M. Lekka, E. Marin and L. Fedrizzi, 'Tribological Behavior of Thermal Spray Coatings, Deposited by HVOF and APS Techniques, and Composite Electrodeposits Ni/SiC at Both Room Temperature and 300 °C', *Tribology in Industry*, vol. 35, no. 2, pp. 113-122, 2013.

[24] K. Sairama, J.K. Sonber, T.S.R.Ch. Murthy, C. Subramanian, R.K. Fotedar, P. Nanekar and R.C. Hubli, 'Influence of spark plasma sintering parameters on densification and mechanical properties of boron carbide', *Int. J. Refract. Met. Hard Mater.*, vol. 42, pp. 185–192, 2014.

[25] Z. Guimin, W. Yucheng, F. Zhengyi, W. Hao, W. Weiming, Z. Jinyong and Z. Qingjie, 'Synthesis of Mullite at low temperature and its chemical composition', *J. Chin. Ceram*., vol. 36, pp. 1542-1547, 2008.

[26] D. Jianxin, D. Zeliang, Z. Jun, L. Jianfeng and C.Tongkun, 'Unlubricated friction and wear behaviors of various alumina-based ceramic composites against cemented carbide', *Ceram. Int.*, vol. 32, no. 5, pp. 499-507, 2006.

[27] O. Hiroshi, K. Toshi, N. Atsushi and K. Niihara, 'Microstructure and Mechanical Properties of Mullite Ceramics', *J. Ceram. Soc. Jpn*., vol. 98, no. 1138, pp. 541–547, 1990.

[28] M. Ismail, N. Zenjiro and S. Shigeyuki, 'Microstructure and Mechanical Properties of Mullite Prepared by the Sol-Gel Method', *J. Am. Ceram. Soc.*, vol. 70, no. 1, pp. C7–C8, 1987.

[29] K. Hidehiro, S. Hisao and I. Takahiro, 'Densification of Sol-Gel-Derived Mullite Ceramics after Cold Isostatic Pressing up to 1 GPa', *J. Am. Ceram. Soc*., vol. 81, no. 1, pp. 173–179, 1998.

[30] S.W. Wang, L.D. Chen and T. Hirai, 'Densification of Al_2O_3 Powder Using Spark Plasma Sintering', *J. Mater. Res.*, vol. 15, no. 4, pp. 982–987, 2000.

[31] K. Hiroshi, 'Science and New Applications of Electric Discharge Consolidation', *J Jpn Soc Powder Powder Metall*, vol. 45, no. 11, pp.1050–1054, 1998.

[32] T. Masao, 'Trends in Advanced SPS Spark Plasma Sintering Systems and Technology. Functionally Gradient Materials and Unique Synthetic Processing Methods from Next Generation of Powder Technology', *J. Soc. Powder Technol.*, vol. 30, no. 11, pp. 790–804, 1993.

[33] M. I. Osendi and C. Baudin, 'Mechanical Properties of Mullite Materials', *J. Eur. Ceram. Soc.*, vol. 16, no. 2, pp. 211-224, 1996.